RESEARCH ARTICLE

Classification of Spermatogenic Cells in *Rana tigerina* Based on Ultrastructure

Sirikul Manochantr, Prapee Sretarugsa, Chaitip Wanichanon, Jittipan Chavadej and Prasert Sobhon*

Department of Anatomy, Faculty of Science, Mahidol University, Rama VI Road, Bangkok 10400, Thailand.

* Corresponding author, Email: scpso@mahidol.ac.th

ABSTRACT: Germ cells in the spermatogenetic process of *Rana tigerina* can be classified into 14 steps based on the pattern and degree of chromatin condensation as studied by transmission electron microscopy. Primary spermatogonia contain a large spherical nuclei with mostly euchromatin that consists of 2 levels of fibers with 10 and 30 nm thicknesses. Secondary spermatogonia have small heterochromatin blocks consisting of tight aggregations of 30 nm fibers on the inner surface of the nuclear envelope, as well as in the central area of the nucleus. Primary spermatocytes are divided into 6 steps. A leptotene spermatocytes contain small loosely packed chromatin clumps that are resulted from the winding of 30 nm fibers around the condensation axes, each of which is a single electron dense line. Zygotene spermatocytes contain long and increasingly thickened heterochromatin blocks, which are joined together by synaptonemal complexes. Pachytene spermatocytes show long, thick, intertwined heterochromatin blocks cords, which are parts of the complete chromosomes. These chromatin blocks become distributed in a cartwheel pattern in diplotene spermatocytes. Long and large heterochromatin blocks are separated from each other during the diakinesis step and become aligned along the equatorial region in the metaphase spermatocytes. Throughout the transformation of primary spermatocytes, the 30 nm chromatin fibers become increasingly condensed into heterochromatin blocks of various sizes, while the 10 nm fibers are decreased in quantity until they are absent entirely in the metaphase spermatocytes. Secondary spermatocytes have nuclei that contain 4-6 large blocks of heterochromatin along the inner facet of the nuclear envelope, the 30 nm fibers are loosened up and the 10 nm fibers of which start to reappear. Spermatids can be divided into 4 steps. In spermatid I, the nucleus is round and contains more dispersed 30 nm chromatin fibers that are unraveled from the more tightly packed chromatin of the secondary spermatocytes. The 30 nm chromatin fibers are uniformly packed together and increasingly condensed in spermatid II, whose nucleus is decreased in size and becoming oval shaped. In spermatid III, the nucleus becomes elongated and it contains 30 nm chromatin fibers which are aggregated more tightly and evenly together, while 10 nm fibers disappear. In spermatid IV, the nucleus becomes highly elongated into a cylindrical shape, with a small acrosome covering the anterior pole. Its chromatin is highly condensed, but the outline of the 30 nm fibers could still be observed. In spermatozoa, the 30 nm chromatin fibers are packed so tightly together that chromatin becomes completely electron-opaque. The condensation of chromatin in *Rana* spermatozoa is, therefore, similar to the process of heterochromatization in fully differentiated somatic cells, where 30 nm fibers coalesce together without changing their initial size.

KEYWORDS: *Rana tigerina*, spermatogenic cells, ultrastructure, chromatin organization.

INTRODUCTION

During spermatogenesis and spermiogenesis of vertebrates, the chromatin undergoes extensive molecular reorganization and condensation that renders it more compact and metabolically inert as all paternal genes are switched off, and the chromatin must be contained within the highly reduced volume of the sperm nucleus.[1,2] Thus, the paternal genome is protected against physical damage and chemical mutagenesis during transport to the site of fertilization.[3] Changes in basic proteins complexed with the DNA are of particular interest and have long been regarded as an important contributing factor to variations in the chromatin packaging pattern.[4] The process of chromatin condensation has been well studied in mammalian spermatozoa,[5-7] and at least two patterns of chromatin condensation can be discerned.[7,8] In primates including human, the fine granular chromatin substance of early spermatids is gradually replaced by coarser and denser bodies, which appear to arise by the "growing" or "aggregating" of smaller dispersed chromatin granules.[7,9,10] The chromatin bodies increase in size and eventually

coalesce to form the compact homogenous mass of the typical chromatin in the mature spermatozoa.[7, 11] Alternatively, in most rodents the basic nucleosomal-type, the 30 nm chromatin fibers, are transformed into larger (40-50 nm) fibers that are straight and arranged in parallel during the early acrosomal stage.[12] These fibers appear to grow larger by the lateral fusion of the smaller parallel fibers, until they reach about 100 nm in width. Later the large fibers are completely fused to form the compact chromatin.[12] While early round spermatids (Golgi and cap phases) contain a mixture of somatic types as well as testis-specific histones, these proteins are largely replaced by a set of novel transition proteins (TP) about midway through spermiogenesis (acrosomal stage),[5] when the chromatin appears as 40-50 nm straight parallel fibers.[12] Shortly thereafter (maturation stage), the transition proteins are replaced by the arginine-rich protein, protamine, which are responsible for the final compaction of chromatin in the mature sperm head.[13] The pattern of chromatin condensation is thus highly correlated with the steps of germ cell development, especially during spermiogenesis. Only a limited amount of information is available on the process of spermatogenesis and the organization of chromatin in amphibians, and none is available in *Rana tigerina,* a species of rice field frogs which is indigenous to Thailand. Thus, the purposes of the present study are to classify various steps of the development of male germ cells in *Rana tigerina* based on the pattern of chromatin organization and ultrastructural features.

MATERIALS AND METHODS

Experimental Animals

Rana tigerina, rural rice field frogs commonly found in Thailand, were cultured in cement tanks at the Faculty of Science, Mahidol University. They were maintained in a natural environment having approximate 12 hour light/dark cycle. The ambient temperature was about 25-30 °C, while the relative humidity ranged from 80 to 100%. Pelleted frog feeds were given once daily in the afternoon, and the water in the cement tanks was changed at alternate days. Only sexually mature frogs, generally more than 12 month-olds,[14] were used in the experiment.

Specimen Preparation

Mature male frogs that were more than 12 months old were collected during the breeding season (April-October),[14] and anesthesized by being placed in an ice bath for 5-10 minutes, or until they become immobile. The testes were removed and immediately processed for transmission electron microscopy. The testicular tissues were cut into small pieces about 1 mm^3 and

fixed in the solution of 4% glutaraldehyde plus 2% paraformaldehyde in 0.1 M Millonig's buffer (0.23 M $NaH_2PO_4.H_2O$, 0.19 M NaOH, 0.06 M glucose), pH 7.2, at 4 ^{o}C for 2 hours. Then the tissues were washed in three changes of the same buffer in order to remove the fixatives, followed by post fixation in 1% osmium tetroxide in the same buffer for 1 hour. Then, the tissues were washed again in three changes of the same buffer. After fixation, specimens were dehydrated through increasing concentrations of ethyl alcohol at 50%, 70%, 90% and 95%, consecutively, by immersing them for 10 minutes, twice at each ethanol concentration, and at 100%, by immersing them for 20 minutes, 3 times, at 4 ^{o}C and 20 minutes, 3 times, at room temperature. Then the specimens were cleared in two changes of propylene oxide, for 15 minutes each, infiltrated in mixtures of propylene oxide and Araldite 502 resin at the ratios of 2:1 for 1 hour, and 1:2 overnight, then in pure Araldite 502 resin for at least 6 hours, and finally polymerized at 30 ^{o}C, 45 ^{o}C and 60 ^{o}C for 24, 48 and 48 hours, respectively.

Light Microscopy

In order to facilitate the classification of various steps of male germ cells, thick sections of about 0.75-1 mm were cut from each blocks of Araldite-embedded tissue with glass knives on a Porter-Blum MT-2 ultramicrotome, mounted on glass slides at 55 ^{o}C, and stained with 1% methylene blue in 1% borax in H_2O at 70 ^{o}C, for 30 seconds, washed with several changes of distilled water, then dried on a hot plate and covered by glass cover slips using superglue as the mounting medium. The sections were examined and photo-graphed with an Olympus Vanox microscope.

Transmission Electron Microscopy

Thin sections with an interference color of silver to silver-gold (about 60-90 nm thick) were cut with glass knives on a Porter-Blum MT-2 ultramicrotome. The sections were picked up on uncoated 300-mesh copper grids, air dried and stained by floating on saturated aqueous uranyl acetate in the dark for 30 minutes, then rinsed with several changes of distilled water, and the excess water was blotted off with Whatmann filter paper. The sections were further stained by floating on saturated aqueous lead citrate for 30 minutes, rinsed with several changes of CO_2-free distilled water, and the excess water blotted off with Whatman filter paper and air dried. The sections were then examined with a Hitachi transmission electron microscope H-300 at 75 kV.

Scanning Electron Microscopy

Spermatozoa collected from cloaca were fixed in the solution of 4% glutaraldehyde plus 2%

paraformaldehyde in 0.1 M Millonig's buffer, pH 7.2 at 4 °C for 1 hour, the specimen were then washed in three changes of the same buffer, 5 minutes each, followed by post fixation in 1% osmium tetroxide in the same buffer for 30 minutes. Then, the specimen were washed again in three changes of the same buffer. After fixation, specimens were dehydrated through an increasing concentrations of ethyl alcohol at 50%, 70%, 90%, and 95% consecutively, by immersing them for 10 minutes, twice at each ethanol concentration and at 100 %by immersing them for 10 minutes for 3 times, at 4 °C. Specimens were dried in a Hitachi HCP-21 critical-point drying machine, using liquid CO_2 as a transitional medium. They were mounted on aluminum stubs with carbon-paint adhesive, and coated with platinum and palladium in a Hitachi ion sputtering apparatus, E2500. The specimens were examined by a Hitachi S-2500 scanning electron microscope at 15 kV.

Measurement of Chromatin Fibers

The male germ cells of *R. tigerina* were classified into various steps based on the pattern of chromatin organization and other ultrastructural features including the acrosome and the tail formation. The sizes of chromatin fibers in at least 10 cells from each step of the male germ cells were measured from electron microscopic negatives in a Nikon profile projector. Fibers were measured at random by recording the distance between the distinct edges. Catalase crystal with lattice spacing of 87.5 Å (Agar Aids) was photographed at the same magnifications and used as standards for measurement of chromatin fiber sizes. From the variation in sizes and the orientation of the chromatin fibers, the patterns of chromatin organization and condensation was deduced.

RESULTS

Histological Organization of *Rana tigerina* Testis

Each testicular lobule contains several convoluted seminiferous tubules, each of which is surrounded by a thick basement membrane. The seminiferous epithelium consists of 2 groups of cells, i.e., spermatogenic cells and follicular cells (Fig 1A). The interstitial areas are filled with interstitial cells, blood vessels and connective tissues (Fig 1A). The differentiating male germ cells are always found in synchronously developing groups, each surrounded by processes of follicular cells, thus this structure is called a spermatocyst (Fig 1A). Because of this unique organization, the steps of spermatogenic cells could be clearly identified. At the beginning of the spermatogenic process, the spermatocyst consists of a single large primary spermatogonium enclosed in a layer of follicular cells (Fig 1B). The primary spermatogonium gives rise, by successive mitotic division, to a number of secondary spermatogonia (Fig 1C). These differentiate into six steps of primary spermatocytes (Figs 1B-F) that finally undergo meiotic division to form secondary spermatocytes (Fig 1E). These cells, in turn, undergo a second meiotic division, giving rise to double the number of spermatids (Figs 1G-I). As a result of these divisions, the size of the spermatocyst is increased considerably, and the processes of enveloping follicular cells become highly attenuated (Figs 1A-I). The spermatids are elongated, and oriented in clusters embedded in the cytoplasm of follicular cells (Fig 1I). Thus, it appears that follicular cells of the spermatocysts serve the same sustentacular and nutritive function as the Sertoli cells of mammalian testis.[15] The wall of the spermatocyst ultimately breaks down, leaving the follicular cells and their adhering clusters of spermatids and spermatozoa still attached to the basement membrane of the seminiferous tubule (Fig 1I).

Classification of Spermatogenic Cells

Based on the nuclear size and the pattern and degree of chromatin condensation, and in later stages, the formation of the acrosome and the tails, spermatogenic cells of *Rana tigerina* can be classified into 14 steps.

Primary spermatogonium (Sg1)

This cell contains a large spherical nucleus about 8-10 µm in diameter with mostly euchromatin with very few blocks of heterochromatin in the center. Each nucleus contains one or two prominent nucleoli (Figs 1B, J). The chromatin consists of 2 levels of fibers with about 10 and 30 nm in diameter. The former appear as thin zigzag lines, while the latter appear in cross sections as dense dots (Fig 1L). Small heterochromatin blocks, which are formed by tight aggregation of 30 nm fibers, are few in number and widely scattered throughout the nucleus (Fig 1L). The cytoplasm contains a little developing rough endoplasmic recticulum (Figs 1J, K). Polyribosomes are numerous and evenly distributed throughout the cytoplasm, whereas mitochondria tend to be congregated in one pole of the cell (Fig 1J). Some of these cells are undergoing mitotic division as the two newly divided nuclei remain within the same cytoplasmic mass (Fig 1K).

Secondary spermatogonium (Sg2)

These cells appear in clusters of 2 or 4 cells, still lying close to the basement membrane, and each cluster is surrounded by processes of follicular cells to form a cyst (Fig 1C). The nucleus of Sg2 is round and has a diameter of about 6-7 µm. The nucleoli
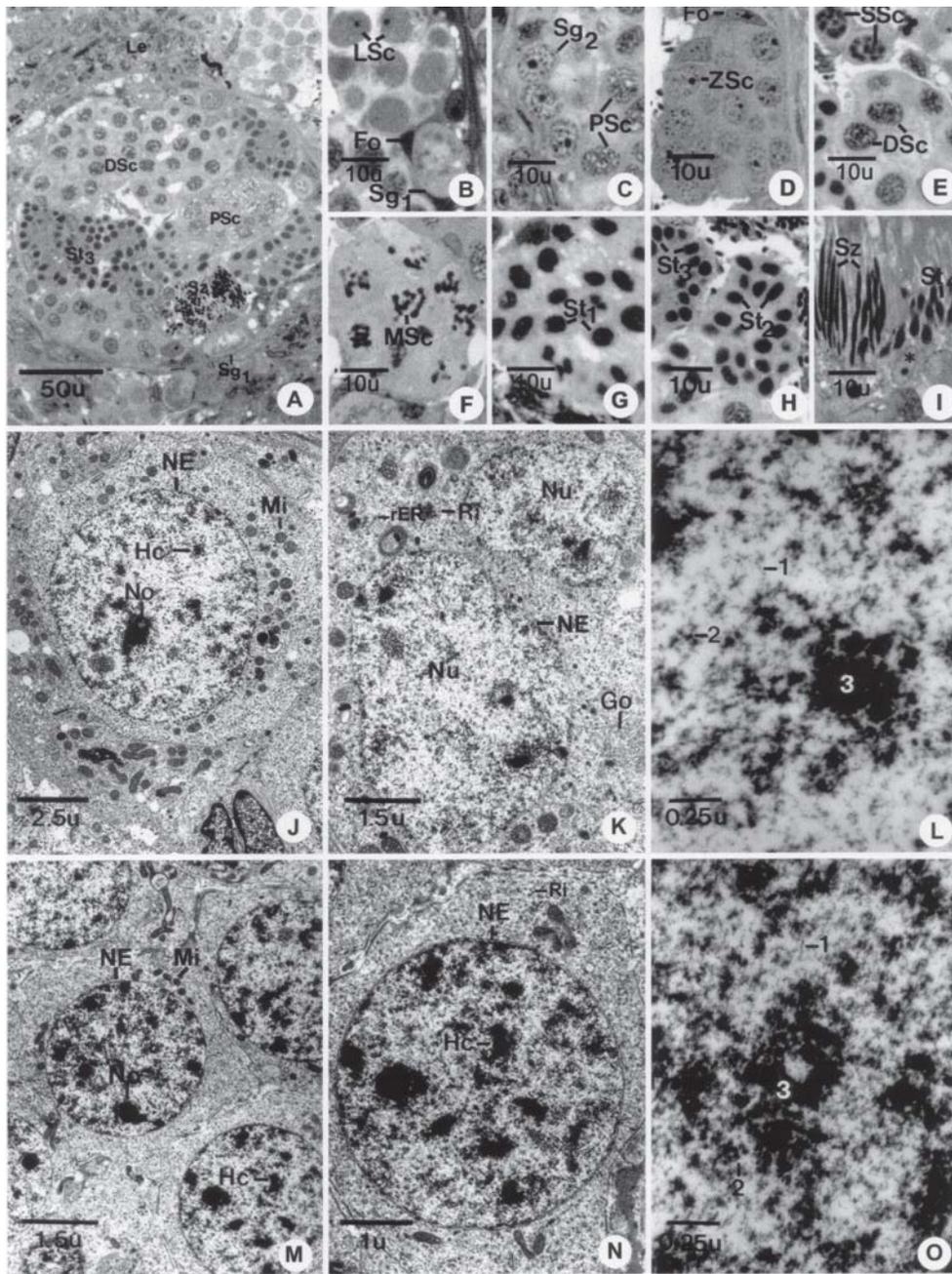
Fig 1.

A-I   Semithin sections of a frog's testis showing the histology of seminiferous tubules and the spermatocysts containing clones of synchronously developing male germ cells: primary spermatogonia (Sg1), secondary spermatogonia (Sg2), leptotene spermatocyte (LSc), zygotene spermatocyte (ZSc), pachytene spermatocyte (PSc), diplotene spermatocyte (DSc), metaphase spermatocyte (MSc), secondary spermatocyte (SSc), spermatid I (St1), spermatid II (St2), spermatid III (St3), spermatid IV (St4) and spermatozoa (Sz). Each spermatocyst surrounded by the processes of follicular cell (Fo). The interstitial area are filled with interstitial Leydig cells (Le). Star (*) indicates the Sertoli cell.

J-L   Transmission electron micrographs of primary spermatogonia (Sg1): the nucleus (Nu) contains mostly euchromatin, which consists of 2 levels of fibers, 10 and 30 nm in width (1, 2). Tight aggregations of 30 nm fibers (3) form heterochromatin blocks (Hc). The cytoplasm contains few endoplasmic recticulum (rER), Golgi complex (Go), numerous ribosomes (Ri) and mitochondria (Mi).

M-O   Secondary spermatogonia (Sg2): Small heterochromatin blocks (Hc) are increasing in number and scattered throughout the nucleus. Chromatin fibers are organized into 2 levels as in primary spermatogonia. The cytoplasm contains abundant ribosomes (Ri), and mitochondria (Mi).

become more prominent (Figs 1C, 1M). The nucleus contains increasing number of small blocks of heterochromatin compared to Sg1, which are distributed along the inner facet of nuclear envelope as well as in the central region (Fig 1N). In the euchromatic area, chromatin fibers are organized into 2 levels, i.e., 10 nm and 30 nm, like in Sg1 (Fig 1O). Cytoplasm contains abundant polyribosomes, fewer mitochon-dria than in Sg1, and rough endoplasmic reticuli which is fairly evenly distributed throughout the cytoplasmic mass (Figs 1M , 1N).

Primary spermatocytes

There are 6 steps of primary spermatocytes: leptotene, zygotene, pachytene, diplotene, diakinesis and metaphase steps, each with distinctive patterns of chromatin organization.

Leptotene spermatocyte (LSc)

The cells in this step are grouped in a large cluster of more than four cells per group, each surrounded by cytoplasmic processes of follicular cells (Fig 1B). The LSc is spherical in shape, with a large spherical nucleus about 6-8 mm in diameter (Fig 2A). Most of the chromatin is in the euchromatic form (Fig 2B), and there is no thin rim of condensed chromatin along the nuclear envelope as observed in earlier steps of spermatogenesis. Small loosely packed chromatin blocks are scattered among the evenly dispersed 30 nm fibers (Fig 2B). In the euchromatic area, individual chromatin fibers exhibit two levels of organization, i.e., 30 nm fibers that appear in cross sections as dense dots, and 10 nm fibers that appear as zigzag thin lines (Fig 2C). Within each enlarging chromatin block in the nucleus of late LSc, where chromatin fibers begin to wind together, there is a dense line that may be the initial site of chromatin condensation (Figs 2E, 1F). The nucleolus is still present but not as prominent as in spermatogonia (Figs 1B , 2A). In addition to abundant ribosomes and mitochondria, the cytoplasm also contains small Golgi complexes (Figs 2A , 2D).

Zygotene spermatocyte (ZSc)

This cell has a round nucleus with approximately the same size as LSc. The distinguishing feature of ZSc is the increase in size and density of heterochromatin blocks, some of which are coupled with the synaptonemal complex (Figs 2G, 2H). In contrast to the single dense line found in LSc, each of this tripartite structure has a conspicuous central element separated from the two lateral elements by clear spaces (Fig 2I). Chromatin fibers (30 nm) from sister chromatids are attached to the side of each lateral element of the synaptonemal complex (Fig 2I). The nucleolus completely disappears. Polysomes appear to be less numerous than in spermatogonial cytoplasm (Figs 2G, 2H).

Pachytene spermatocyte (PSc)

The nucleus of this cell is still round and about 6-7 μm in diameter (Figs 1C, 3A). It is characterized by the presence of long interconnecting blocks or cords of heterochromatin, some of which are attached at the ends to the nuclear envelope (Figs 3A , 3B). Some of these cords are still linked by synaptonemal complex (Figs 3A , 3B). In euchromatic area there are still 2 levels of chromatin fibers. Individual chromatin fibers within the condensed blocks of heterochromatin could be visualized as having 30 nm in size, even though they are tightly packed together (Fig 3C). The number of cells in each cluster increases, and each cluster is still enclosed by cytoplasmic processes of follicular cells (Fig 1C). PSc are the most numerous cell type in the seminiferous tubule and easily observed due to their unique characteristics as mentioned. The cytoplasm also contains ribosomes, mitochondria, and rough endoplasmic recticulum (Fig 3A).

Diplotene spermatocyte (DSc)

The nucleus of this cell has a round to oval shape with slightly smaller size than PSc (about 5-6 mm in diameter). The chromatin blocks become increasingly larger and attached to the nuclear envelope in a cartwheel-spoke pattern (Figs 1E , 3D). Despite the much increased condensation, individual 30 nm chromatin fibers within the tight aggregates of heterochromatin blocks could still be visualized (Fig 3F). There are fewer 10 nm fibers remaining in the euchromatic areas in comparison to PSc (Figs 3E , 3F). DSc are much fewer in number than PSc. The types and quantity of cytoplasmic organelles appear similar to those of PSc (Fig 3D).

Diakinesis-Metaphase spermatocytes (DiSc, MSc)

DiSc is identified by the presence of long and large pieces of chromosomes that are distributed within the whole nucleus (Fig 3G). DiSc rapidly turns into MSc whose chromosomes become aligned in a row along the equatorial region (Fig 3H). The nuclear membrane disintegrates and completely disappears in MSc (Fig 3H). Despite their tight aggregation, the outline of individual 30 nm chromatin fibers in the chromosomes could still be visualized, while the 10 nm chromatin fibers disappear (Fig 3I). The cytoplasm contains only a few organelles, mainly, ribosomes and mitochondria (Fig 3G). Both DiSc and MSc are so few and transient that they are only occasionally observed within the seminiferous tubule. Thus, it could be concluded that throughout the transformation of primary spermatocytes, 30 nm chromatin fibers become increasingly condensed into larger heterochromatin blocks, while still maintaining their individual identity, and the 10 nm fibers are decreasing in quantity until they are entirely absent in MSc (Fig 3I).
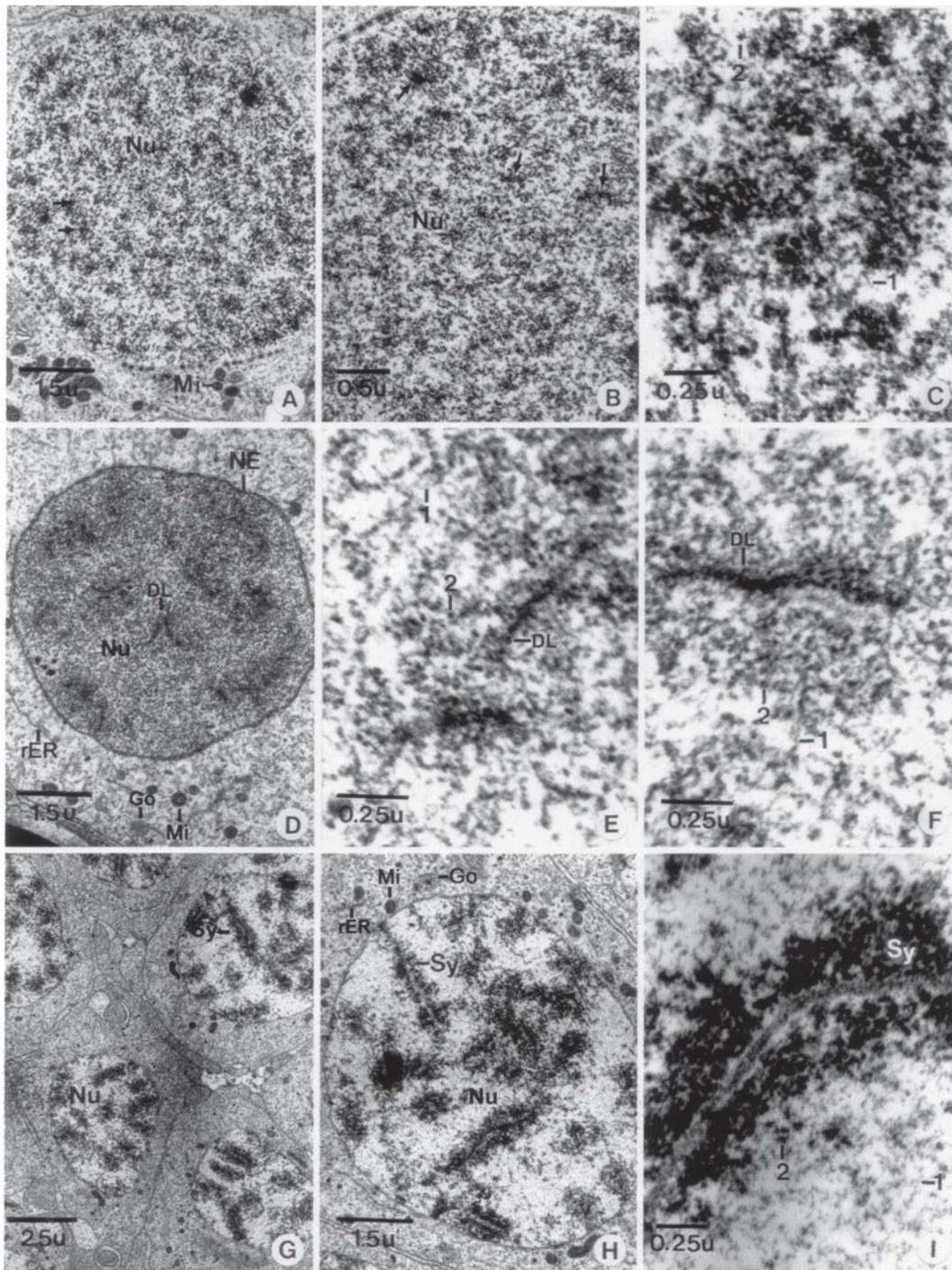
Fig 2.

A-C   Early leptotene spermatocytes (LSc): the nucleus (Nu) has a round shape. It contains 10 nm (1) and 30 nm (2) chromatin fibers. Small blocks of condensed chromatin (arrow) are evenly scattered throughout the nucleus.

D-F   Late leptotene spermatocytes (LSc): the dense line (DL) can be identified as a single long thick line in the nucleus (Nu), where 30 nm (2) chromatin fibers are threaded together and start condensing into a larger heterochromatin block. The cytoplasm contains mitochondria (Mi) and rough endoplasmic recticulum (rER).

G-I   Zygotene spermatocytes (ZSc): in the nucleus (Nu), the synaptonemal complex (Sy) is fully formed and become numerous. Chromatin fibers are still organized into 2 levels, i.e., 10 nm (1) and 30 nm (2). The cytoplasm contains mitochondria (Mi), Golgi complex (Go) and rough endoplasmic recticulum (rER). High magnification of the synaptonemal complex is displayed in Fig I.
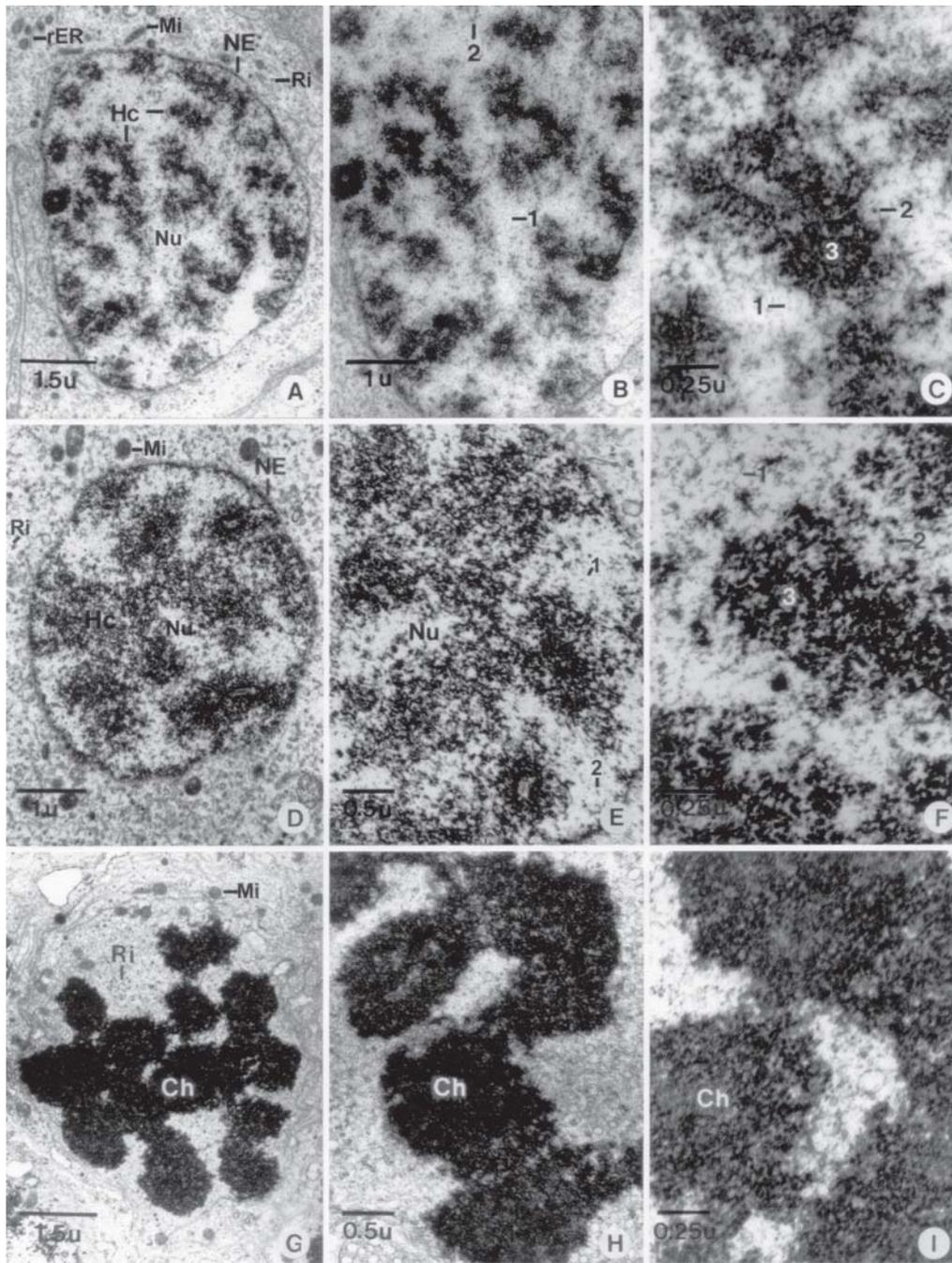
Fig 3.

A-C Pachytene spermatocytes (PSc): the nucleus (Nu) exhibits long and thick intertwined heterochromatin blocks or cords (Hc). Chromatin fibers can be identified as 2 levels, and those within the heterochromatin blocks could still be visualized individually as 30 nm fibers (3). The cytoplasm contains mitochondria (Mi), ribosome (Ri) and rough endoplasmic recticulum (rER).

D-F Diplotene spermatocytes (DSc): the nucleus (Nu) shows long and thick heterochromatin blocks (Hc) aligned along the nuclear envelope (NE) in a cartwheel pattern. Most single chromatin fibers are 30 nm (2) in size while 10 nm fibers (1) are much decreased in quantity. The cytoplasm contains mitochondria (Mi) and ribosomes (Ri).

G-I Diakinesis-metaphase spermatocytes (DiSc-MSc): the nucleus exhibits 30 nm chromatin fibers aggregated together to form long and large chromosomes (Ch) that begin to separate from each other in the diakinesis step (in G), and move to be aligned along the equatorial region in the metaphase step (in H). Only 30 nm fibers are present, within the chromosomes, whose outlines could still be visualized (in I). The cytoplasm contains only a few organelles, mainly mitochondria (Mi) and ribosome (Ri).

Secondary spermatocyte (SSc)

The first meiotic division of a primary sperma-tocyte generates two secondary spermatocytes. It is seldom observed in a histological section, implying that duration of a spermatogenic cell in the secondary spermatocyte step is relatively short. The nucleus of a secondary spermatocyte is round, about 5-6 μm in diameter (Figs 1E, 4A). It contains 4-6 large clumps of heterochromatin blocks along the inner facet of the nuclear envelope, usually with one block in the center (Fig 4A). The 30 nm fibers within the heterochromatin blocks are loosely packed in contrast to those appearing in late spermatocytes (PSc and DSc); and 10 nm fibers become visible again (Figs 4B, 4C). The cytoplasm has similar features to that in the earlier steps, but with an increasing number of vacuoles (Fig 4A).

Classification of Spermiogenic Cells

There are four steps of spermatids, i.e., spermatid I (St1), spermatid II (St2), spermatid III (St3) and spermatid IV (St4), which could be classified on the basis of nuclear sizes and shapes, the patterns of chromatin condensation, and the degree of acrosome formation. The nuclei of successive steps vary from round to oval, and finally to a cylindrical shape, and range in sizes from 3-4 mm in St1 to 2×6 μm in St4.

*Spermatid I (St1):*These cells are still grouped in cysts that lie close to the lumen (Fig 1G). Each cell is characterized by the presence of a round to oval-shaped nucleus, which is reduced in size to approxi-mately 4-5 μm in diameter (Fig 4D). The nucleus contains loosely coiled 30 nm chromatin fibers that are more evenly spread when compared those in SSc (Figs 4D-4F). The 10 nm fibers appear in the light nucleoplasm between the aggregates of 30 nm fibers (Fig 4F). The cytoplasm is a relatively large mass as the nucleus is reduced in size (Fig 4D). In addition to abundant mitochondria and relatively few ribosome, the cytoplasm also contains few rough endoplasmic reticulum, a few stacks of flattened vesicles of Golgi complex and small, smooth vesicles closely associated with it (Fig 4D).

Spermatid II (St2): The nucleus of St2 is decreased in size and transforms into an oval shape about 3×4 mm in diameter, as well as becoming eccentrically located within the cell (Figs 1H, 4G). The nucleus contains evenly dispersed 30 nm chromatin fibers, which appear in cross sections as dense granules (Fig 4I). Few small heterochromatin blocks, and 10 nm chromatin fibers are still present (Figs 4H, 4I). In the cytoplasm a large Golgi complex, each consisting of 4-5 stacks of cisternae (Fig 4H), is formed on one side of the nucleus while the opposite side exhibits the development of the flagellum, with an axoneme

outgrowing from the basal body (Fig 4G). Pro-acrosomal vesicles of various sizes are distributed near the Golgi complex. Globular-shaped mitochon-dria with tubular cristae are widely dispersed throughout the cell (Fig 4G). The acrosome starts to appear as a short thick but flat segment on the nuclear envelope, at the location adjoining the Golgi complex (Fig 4H). The two leaflets of the nuclear envelope lie close together at acrosomal area, whereas they are more widely and irregularly spaced elsewhere. Underneath the nuclear envelope there is an evenly thick, dense, layer of the nuclear lamina (Fig 4I).

Spermatid III (St3): The nucleus of St3 becomes elongated to about 2x4 μm in size (Figs 1H , 5A). It contains 30 nm fibers which are closely packed together and becomes almost uniformly dense (Fig 5A, B), except in pockets of light areas where there appear to be fewer chromatin fibers (Fig 5B). The 10 nm fibers completely disappear (Fig 5C). The acrosome appears as an enlarged thickened plate in close apposition to the nuclear envelope at one pole of the nucleus (Fig 5B). The cytoplasm is relatively clear in comparison with earlier spermatids, and the cytoplasmic organelles become sparse except for the mitochondria, which appear to be concentrated around the tail (Fig 5A). The cytoplasm shows progressive migration to the caudal part of the nucleus and becomes more elongated (Fig 5A). At the caudal end of the nucleus the centrioles, which are surrounded by a striated cylindrical fibrous sheath, start to form the base of the tail axoneme (Fig 5A). The branches of the striated cylindrical fibrous sheath extend laterally from the side of the centrioles (Figs 5A , 5I).

Spermatid IV (St4): Spermatids 4 usually lie close to the lumen of seminiferous tubule, where the heads are usually embedded in the cytoplasm of folliculo-Sertoli cell (Fig 1I). The nucleus is elongated to about 1.5×7 μm in size (Fig 5D, 5E). The chromatin becomes almost completely condensed throughout the nucleus, as 30 nm fibers, become tightly packed; however, the outlines of individual fibers (granules) are still visible (Fig 5F). The cytoplasm is pushed back to the opposite side to where the acrosome is (Figs 5D, 5E). Only the caudal end still possesses a substantial amount of cytoplasm (Fig 5E). The acrosome appears as a flat cap-like structure over the pointed anterior end of the nucleus. Its interior has a homogeneous matrix of medium density (Fig 5D). The striated cylindrical fibrous sheath, which becomes a part of the initial segment of the midpiece, increases in length and is inserted to the caudal end of the nucleus (Fig 5E). The mitochondria start to cluster around the striated cylindrical fibrous sheath of the initial segment (Fig 5E).

Spermatozoa (Sz): The mature spermatozoa are recognized by their highly elongated cylindrical nuclei, with slightly tapered anterior end (Fig 1I). Each head is about 9-11 mm in length and 0.5-0.75 mm in width at the mid-section (Fig 5G). The nucleus occupies virtually the entire head region which is surrounded by a smooth plasma membrane. It contains completely opaque chromatin with very few intra-nuclear vacuoles (Fig 5H). The 30 nm chromatin fibers are tightly compact into an electron dense mass, such that the outline of individual 30 nm chromatin fibers could no longer be resolved (Figs 5H, 5I). The anterior portion of the nucleus is smoothly curved and covered by a thin acrosome over a distance of approximately 1-1.5 µm of the anterior region. The inner acrosomal membranes covering the head are closely apposed to the nuclear membrane. The acrosome material appears homogeneous and moderately electron-dense (Fig 5H). A small area of the cytoplasm is present only at the posterior region of the head surrounding the caudal pole of the nucleus and the proximal end of the tail, and slimming down in the midpiece that connects the head and the main part of the tail (Fig 5I). The midpiece contains a pair of centrioles oriented at right angle to each other (Figs 5I, inset), with the distal centriole aligned in continuity with the axoneme of the tail. The centriolar complex as well as the proximal end of the tail's axoneme is surrounded by a striated cylindrical fibrous sheath (Figs 5I, inset). The approximate width of each striated band and the interval between neighboring bands is about 30 nm (Fig 5I). The neck is, therefore, not clearly separated from the midpiece and they together measured approximately 1.7-1.8 µm long from the anterior edge of the proximal centriole to the posterior end of the distal centriole (Fig 5I). The cytoplasm of the midpiece begins to taper at about 1.5-2.5 mm from the base of the nucleus. The mitochondria in the midpiece are non-helical (Figs G, inset), and most are arranged longitudinally along the centriolar-axonemal core (Fig 5I). The principal piece of the tail consists of the 9+2 axonemal complex as the core, surrounded by a smooth plasma membrane (Fig 5I). The tail is about 35-40 mm in length; thus the total length of a mature spermatozoon is approximately 40-50 µm (Fig 5G).

DISCUSSION

Classification of Male Germ Cells in the Testis of *Rana tigerina*

The first ultrastructural study of an anuran (*Bufo arenarum*) spermatogenesis was published by Burgos and Fawcett,[1] who reported 8 stages of the male germ cells, but did not make a detailed classification of spermatids. The male germ cells in the testes of *Xenopus laevis* were classified into 11 stages.[16] By using autoradiographic technique, it was found that the durations of leptotene, zygotene, pachytene, diplotene and metaphase spermatocytes were 4, 6, 12, 1 and 1 days, respectively, and spermiogenesis was completed within 12 days. As for *Rana* species, 11 stages of male germ cells had been identified in *R. esculenta*,[17] which was comparable to *X. laevis*.[16] However, it was noted that the durations of leptotene spermatocyte and spermiogenesis were longer than in *X. laevis*. In the present study of *R. tigerina*, using a more detailed ultrastructural criteria, especially the characteristics of chromatin organization, we could recognize 14 distinct steps of male germ cells. Another interesting finding is that spermatogenesis in *R. tigerina* is occurs within a cyst-like structure, in which germ cells mature in coordinated clusters as in fish.[18] These clusters of germ cells have also been shown in other anuran species and called "spermatocysts".[1] Evidently, individual spermatogonia divide mitotically several times to produce a pool of daughter cells that remain within a common cyst, walled by the processes of follicular cells. Within any particular cyst, successive generations of daughter cells divide synchronously and develop at a similar rate, so that the cyst always contains an increasing cell number in the same step. In *R. temporaria,* spermatogonia undergo eight mitotic divisions, implying that a single spermatogonium could eventually give rise to a cyst containing well over 200 secondary spermatogonia.[18] In *X. laevis* the number of cell divisions within the secondary spermatogonial cysts is reported to vary between four to eight generations.[16] In rats, there are fewer division cycles, and thus a single spermatogonium produces only 24 cells, which subsequently mature into primary spermatocytes.[19] Therefore, the cystic type spermato-genesis could result in mass production of many more gametes than in mammals, and may be an adaptation feature for the external fertilization in fishes and amphibians, where a large quantity of spermatozoa is needed to compensate for the greater difficulty in gamete union.[18]

Ultrastructural characteristics of various steps of the male germ cells, as revealed by transmission electron microscopic studies, help to confirm the classification of male germ cells by light microscopy, as well as to understanding of the cellular activities. A primary spermatogonia (Sg1) have a nuclei, constituted mainly of the euchromatin. This results in very clear nucleoplasm and very prominent nuclei. This suggests high transcriptional activity and a high rate of ribosome synthesis. Each cell divides mitotically, giving rise to secondary spermatogonia (Sg2), which are distinguished by the increasing amount of small heterochromatin blocks. These cells, therefore, may
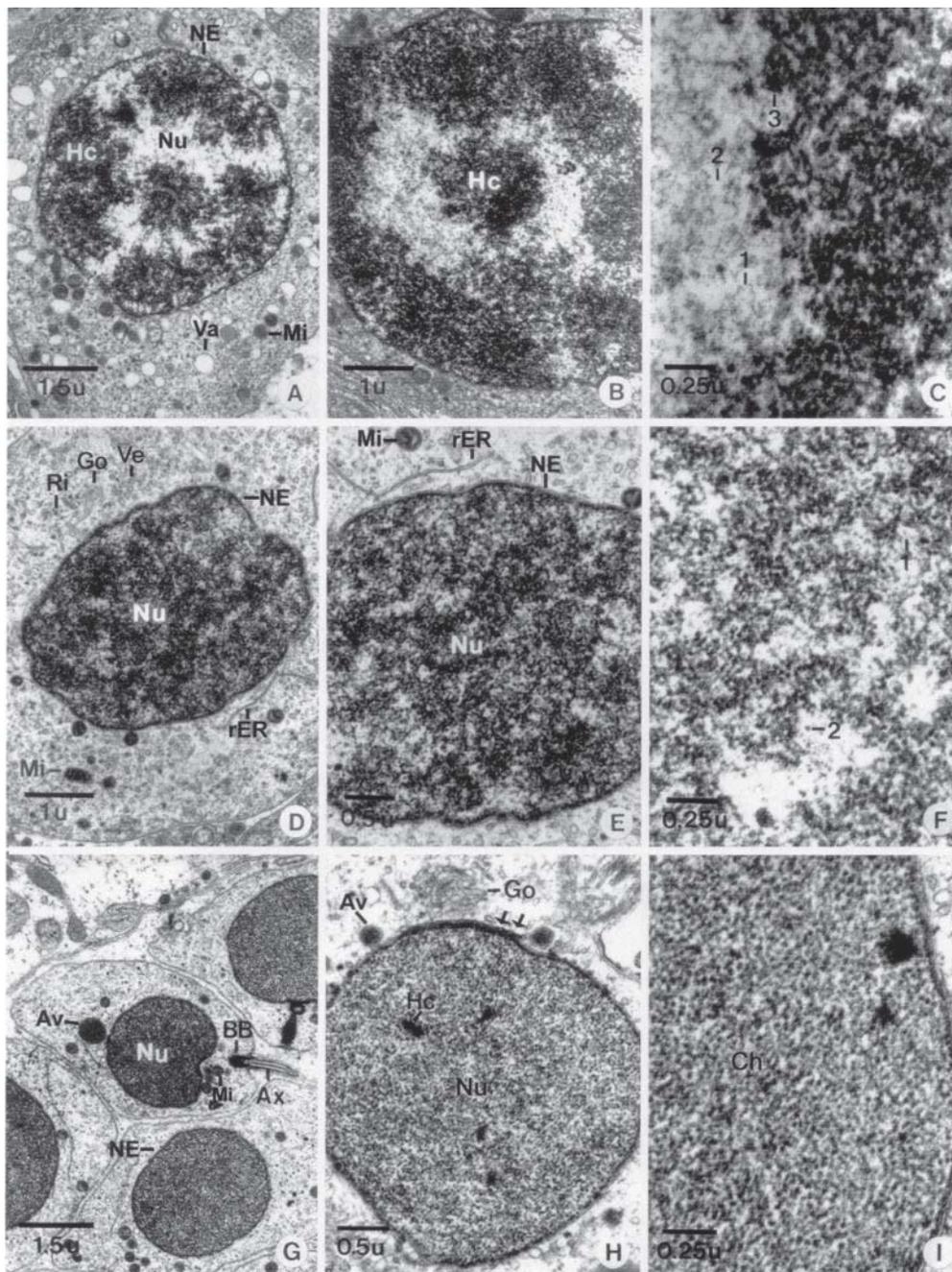
Fig 4.

A-C Secondary spermatocyte (SSc): the nucleus (Nu) contains 4-6 blocks of heterochromatin (Hc) that are distributed on the inner facet of the nuclear envelope (NE). Chromatin fibers could be observed at 2 levels, i.e., 10 nm (1) and 30 nm (2). The heterochromatin (3) is formed from loosely bound 30 nm fibers. The cytoplasm contains numerous mitochondria (Mi) and some vacuoles (Va).

D-F Spermatid I (St1): the nucleus (Nu) has a round shape, and it contains chromatin appearing as fine granules, which are the cross sections of 30 nm fibers (2), and become loosely packed throughout the nucleus. The cytoplasm contains mitochondria (Mi), relatively few ribosomes (Ri), rough endoplasmic recticulum (rER) and a few stacks of Golgi complex (Go) with smooth vesicles (Ve) associated with it.

G-I Spermatid II (St2): the nucleus (Nu) becomes oval shape, in which 30 nm fibers (2) are loosely but evenly packed together, and dispersed uniformly throughout the nucleus (Nu). The Golgi complex (Go) and acrosomal vesicles (Av) are present in the anterior end of the nucleus and the acrosome appears as a short thickening of the nuclear envelope (arrow), while the developing tail appears as an axoneme (Ax) growing out from the basal body (BB) at the posterior end.
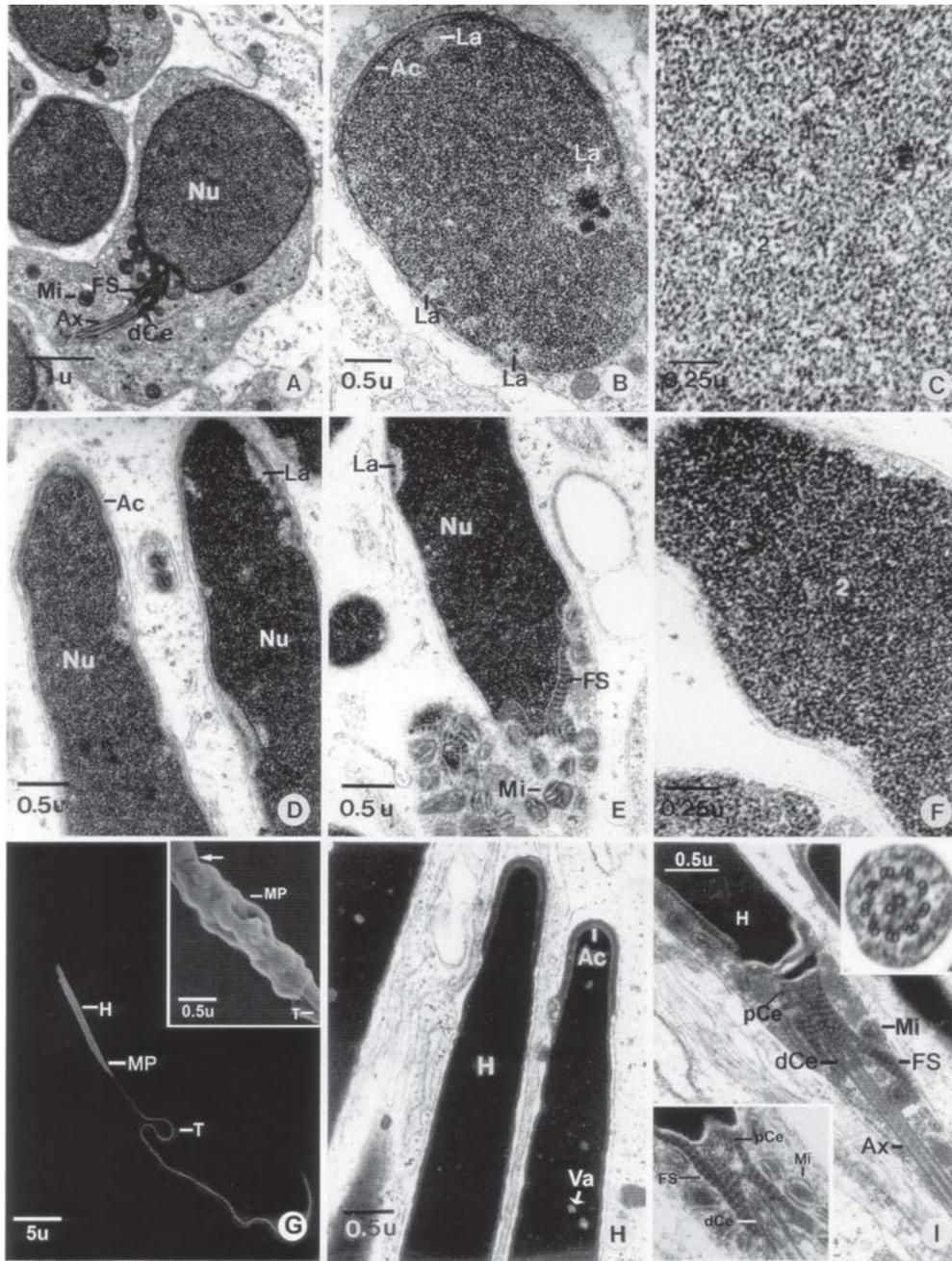
Fig 5.

A-C   Spermatid III (St3): the nucleus (Nu) becomes elongated and 30 nm fibers (2) are closely packed together. Due to the increased condensation of chromatin in most part some lightly stained areas (La) within the nucleus that contain fewer chromatin fibers appear. Fibers at 10 nm disappear completely. the flat acrosome (Ac) and proximal end of the tail consisting of striated cylindrical fibrous sheath (FS), distal centriole (dCe) and axoneme (Ax) are present.

D-F   Spermatid IV (St4): the nuclear elongation is more pronounced while 30 nm fibers (2) become tightly packed, but the outlines of individual fibers are still visible (in F). Lightly stained area (La) are also observed. The caudal end of nucleus contains a striated cylindrical fibrous sheath (FS) and numerous mitochondria (Mi).

G-I   G is the scanning electron micrograph of a spermatozoon: the head (H) has a long cylindrical shape, the tail is very long and flimsy (T) and the middle piece (MP) connects the head and the tail. In TEM micrographs (H, I): the head (H) contains completely condensed and electron opaque chromatin. Only a few vacuoles (Va) are present. A small U-shaped acrosome (Ac) can be observed over the anterior end of the nucleus (in H). The proximal end of the tail consists of a pair of perpendicularly orientated centrioles (pCe, dCe) surrounded by the striated cylindrical fibrous sheath (FS) with rootlets. the axoneme (Ax) growing out from the distal centriole. Mitochondria (Mi) surround the fibrous sheath.

have lower transcriptional activity and lower ribosomal synthesis. In other words they may serve primarily as the means to increase the number of early germ cells, as well as the transient steps to primary spermatocytes. The latter then pass through six steps of the first meiotic division, as observed in vertebrate primary spermatocytes.[19] The nuclear volume of LSc starts to increase again compared to Sg2, due to the need to accommodate the increased amount of duplicated chromosomic DNA. When this process is accomplished, the chromatin fibers appear to wind around the dense axes which make their first appearance in late LSc. These dense axes may be the initial site of chromosome condensation or they could later turn into the synap-tonemal complexes which are responsible for the pairings of homologous chromosomes in ZSc. From then on, chromatin fibers are packed more tightly into heterochromatin blocks that transform into larger cords that are increasingly thickened and lengthened in PSc and DSc. Apparently, due to the chromatin condensation transcriptional activity could cease and ribosomal synthesis is lessened, as reflected the disappearance of the nucleoli in PSc. Furthermore, the cytoplasmic organelles, especially ribosomes and mitochondria are drastically decreased, resulting in a much paler stained cytoplasm. Finally, in the DiSc and MSc steps, the chromatin appears as large pieces of condensed chromosomes that are translocated to the equatorial region. The SSc is the cell after the first meiosis in which the haploid chromosomes start to decondense. Four steps of derived spermatids could be identified based on the nuclear size, shape, and chromatin condensation. The first step exhibits loosely packed 30 nm chromatin fibers, which may become unwound from the SSc step. The chromatin fibers are recondensed into a more even mass in St2 as the nuclear volume decreases. St3 have elongated nuclei, which reflects a beginning of morphogenetic changes of the nuclear shape by a force that is yet to be identified. St4 are characterized by highly elongated, almost cylindrical nuclei, having a higher degree of chromatin condensation, even though each fiber still maintains its individuality and width of 30 nm. Subsequently, the cylindrical-shaped heads together with completely condensed chromatin are observed in spermatozoa. Since the manchette is not observed as in mammalian spermatids, and cells in these steps also show a paucity of cytoskeletal elements, the force that modulates the nuclear shape could be mostly due to chromatin condensation.

The acrosome of *R. tigerina* spermatozoa appears in St 2. It is derived from the Golgi complex, and finally assumes an inverted U-shape of a flattened sheet that adheres tightly to the proximal end of the sperm head. Acrosome formation in *R. tigerina* is different from that in mammals in that very few acrosomal granules and vesicles are formed. This perhaps explains the rather thin and relatively small size of this acrosome as compared to that in mammalian sperm.[20] The large mammalian acrosomes are needed for storage of hydrolytic enzymes, largely hyaluronidase, that are responsible for dispersing the multi-layered cumulus cells. In birds, reptiles and amphibians the ova are not surrounded by this group of cells, hence there is no need for large acrosomes in the sperm of these species.[21]

The cytoplasmic volume and cellular organelles also change during spermatogenesis. Initially in Sg1, there are abundant polyribosomes, flat profiles of rough endoplasmic reticulum, sizable Golgi complexes and numerous small mitochondria. During primary spermatocytes, the numbers of various organelles are reduced, except the Golgi complex, which is quite stable in size and is still observed in spermatids. Much of the cytoplasm is gradually relocated toward the posterior pole, and becomes highly vacuolated in late spermatids, and is mostly cast off in spermatozoa. Some cytoplasm still remains at the midpiece, and this is still quite substantial when compared to that observed in mammalian spermatozoa.[22] The midpiece of *R. tigerina* is of the primitive type, which contains a pair of perpendicular centrioles surrounded by the striated cylindrical fibrous sheath with constant periodicity and rootlet-like structures, as observed in other *Rana* and *Xenopus* species,[23]. This fibrous sheath may help to stabilize and anchor the midpiece to the caudal end of the nucleus. It probably is not involved in the movement (bending) of the tail like the outer fibrous sheath of mammalian sperm.[24] The principal piece is similar to the endpiece of the mammalian spermatozoa, consisting of only an axoneme surrounded by the plasma membrane.[22]

Chromatin Organization in the Male Germ Cells of *Rana tigerina*

During spermatogenesis and spermiogenesis of *R. tigerina,* the chromatin fibers are organized into two fundamental levels, i.e., 10 nm and 30 nm fibers, which are randomly coiled. In LSc, 30 nm fibers appear to wind around a single dense line, which may be the initial part of a chromosome condensation, which becomes enlarged in ZSc (Fig 2G-Fig 2I) and PSc (Fig 3A-Fig 3C). After undergoing the extreme conden-sation into chromosomes to expedite the process of DNA separation in MSc, the 30 nm fibers become loosened again in SSc (Fig 4A-Fig 4C), so that they could eventually be unfolded and become evenly distributed throughout the nucleus in early spermatids (St1, St2) (Fig 4D-Fig 4I); while 10 nm fibers reappear briefly and disappear again in St3 (Fig 5A-Fig 5C). The 30 nm

chromatin fibers, are re-aggregated and packed tightly into a uniformly dense mass in St4, but still remain as individual units (Fig 5D-5F). It is only in the completely opaque mass in spermatozoa that the individuality of 30 nm fibers disappears (Fig 5H). This observation indicates that the 30 nm fibers do not increase in size nor change in conformation during spermatid differentiation. In contrast, in mammals such as rat,[12] primate,[10] human,[7] or even invertebrates such as mollusk,[25] changes in the degree of chromatin condensation occur during the advanced steps of spermiogenesis due to the replacement of histones by the more basic proteins, including protamines or protamine-liked proteins. From the data in this study, it is believed that 30 nm fibers in *R. tigerina* sperm are simply brought close together and coalesced into the complete electron opaque mass. Many studies of mammalian spermiogenesis such as in mouse, rat[12] and human[7] have indicated that the coiled 30 nm fibers occur in the nuclei of early spermatids, and then these fibers transform into larger straight fibers (rodents) or knobby fibers (primates including humans) during the middle and late spermatid steps.[9,10,26] These fibers eventually become tightly packed or fused in spermatozoa. It is believed that the replacement of histones by TP proteins or protamines, the other more basic testis specific proteins, is instrumental in increasing the size of chromatin fibers and their final condensation.[1,5,12] The latter process could be reinforced by the increase of disulfide bond formation among sperm protamines.[7] In contrast, somatic-type histones are found to be present in the mature sperma-tozoal nuclei of *R. pipiens*[27] and *R. catesbeiana*.[28] It has also been shown in the latter that there is no protamine in the spermatozoa, but instead there are H1 variants (H1V) existing together with the full set of core histones. Thus, it was suggested that H1V may play a role in chromatin condensation in the spermatozoa of *Rana* species, instead of protamine-like proteins, as observed in mammalian spermatozoa. H1V may help to aggregate the 30 nm fibers into tight packing, while still maintaining the nucleosomal organization. This type of condensation probably uses the same mechanism that occurs during heterochromatization in fully differentiated cells, such as chick erythrocytes, which use another H1 variant (H5) for initiating the condensation of 30 nm nucleosomal fibers.[29]

ACKNOWLEDGEMENTS

REFERENCES

1. Burgos MH and Fawcett DW (1956) An electron microscope study of spermatid differentiation in the toad, *Bufo arenarum* Hensel. *J Biophysic Biochem Cytol* **2**, 223-240.
2. Reed SC and Stanley HP (1972) Fine structure of spermatogenesis in the South African clawed toad *Xenopus laevis* Daudin. *Ultrastruct Res* **41**, 277-295.
3. Bedford JM and Calvin HI (1974) The occurrence and possible functional significant of –S-S- crosslinks in the sperm, with particular reference to eutherian mammals. *J Exp Zool* **188**, 137-158.
4. Kierszenbaum AL and Tres LL (1978) The packaging unit: A basic structural feature for the condensation of late cricket spermatid nuclei. *J Cell Sci* **33**, 265-283.
5. Oko RJ, Jando V, Wagner CL, Kistler WS and Hermo LS (1996) Chromatin reorganization in rat spermatids during the disappearance of testis-specific histone, H1t, and the appearance of transition proteins TP1 and TP2. *Biol Repro* **54**, 1141-1157.
6. Balhorn R (1982) A model for the structure of chromatin in mammalian sperm. *J Cell Biol* **93**, 298-305.
7. Balhorn R, Cosman M, Thornton K, Krishnan VV, Corzett M, Bench G, Kramer C, *et al* (1999) Protamine mediated condensation of DNA in mammalian sperm. In: *The Male Gamete: From Basic Science to Clinical Applications* (Edited by Gagnon C), pp 55-70. Cache River Press, Vienna, IL.
8. Ward WS, Partin AW and Coffey DS (1989) DNA loop domains in mammalian spermatozoa. *Chromosoma* **98**, 153-159.
9. Holstein AF and Roosen-Runge EC (1981) Atlas of human spermatogenesis. pp 1-224. Berlin Grosse Verlag.
10. Suphamungmee W (2001) Chromatin organization and packaging in the male germ cells of the common tree shew, *Tupaia glis*. M.Sc. Thesis in Anatomy. Faculty of Graduate Studies, Mahidol University.
11. Allen MJ, Bradbury EM and Balhorn R (1997) AFM analysis of DNA-protamine complexes bound to mica. *Nucleic Acids Res* **25**, 2221-2226.
12. Wanichanon C, Weerachatyanukul W, Suphamungmee W, Meepool A, Apisawetakan S, Linthong V, Sretsarugsa P, *et al* (2001) Chromatin condensation during spermiogenesis in rats. *Science Asia* **27**, 211-220.
13. Meistrich ML, Trostle-Weige PK and Van Beek ME (1994) Separation of specific stages of spermatids from vitamin A-synchronized rat testes for assessment of nucleoprotein changes during spermiogenesis. *Biol Reprod* **51**, 334-344.
14. Sretarugsa P, Nakiem V, Sobhon P, Chavadej J, Kruatrachue M and Upatham ES (1997) Structure of the testis of *Rana tigerina* and its changes during development and seasonal variation. *J Sci Soc Thailand* **23**, 75-86.
15. Zhao GQ and Gaebers DL (2002) Male germ cell specification and differentiation. *Devel Cell* **2**:537-547.
16. Kalt MR (1976) Morphology and kinetics of spermatogenesis in *Xenopus laevis*. *J Exp Zool* **195**, 393-408.
17. Rastogi RK, Iela L, Di Meglio M, Di Matteo L, Minucci S and Izzo-Vitiello I (1983) Initiation and kinetic profiles of spermatogenesis in the frog *Rana esculenta* (Amphibian). *Zool Lond* **201**, 515-525.
18. Lofts B (1990) Amphibia. In: *Marshall's physiology of reproduction: Reproductive cycles in vertebrates* (Edited by

Laming GE), pp127-205. Churchill-Livingstone, Edinburgh.

19. Clermont Y and Leblond CP (1953) Renewal of spermatogonia in the rat. *Amer J Anat* **93**, 475-502.

20. Clermont Y and Leblond CP (1955) Spermiogenesis of man, monkey, ram and other mammals as shown by the "periodic acid-Schiff" technique. *Amer J Anat* **96**, 229-50.

21. Cavazos LA and Melampy RM (1954) A comparative study of periodic acid-reactive carbohydrates in vertebrate testes. *Amer J Anat* **95**, 467-90.

22. Jamieson BGM (1999) Spermatozoal phylogeny of the vertebrata. In: *The Male Gamete: From Basic Science to Clinical Applications* (Edited by Gagnon C), pp304-28. Cache River Press, Vienna, IL.

23. Poirier GR and Spink GC (1971) The ultrastructure of testicular spermatozoa in two species of *Rana J Ultrastruct Res* **36**, 455-65.

24. Fawcett DW and Phillips DM (1969) The fine structure and development of the neck region of the mammalian spermatozoon. *Anat Rec* **165**, 153-84.

25. Sobhon P, Apisawetakan S, Linthong V, Pankao V, Wanichanon C, Weerachatyanukul W, Meepool A, *et al* (2001) Ultrastructure of the differentiating male germ cells in *Haliotis asinina* Linnaeus. *Inv Repro Dev* **39**, 55-66.

26. Sobhon P, Tanphaichitr N and Patilantakarnkool M (1984) Transmission and scanning electron microscopic studies of the human sperm heads extracted with 8M urea, 1% mercaptoethanol and different concentrations of salt. *Acta Anat* **120**, 220-7.

27. Zirkin BR (1970) The protein composition and structure of nuclei during spermiogenesis in the leopard frog, *Rana pipiens*. *Chromosoma* **31**, 231-40.

28. Itoh T, Ausio J and Katagiri C (1997) Histone H1 variants as sperm-specific nuclear proteins of *Rana catesbeiana*, and their role in maintaining a unique condensed state of sperm chromatin. *Mol Repro Del* **47**, 181-90.

29. Briand G, Kmiecik D, Sautiere P, Wouters D, Borie-Loy O, Biserte G, Mazen A, *et al* (1980) Chicken erythrocyte histone H5. *FEBS Lett.* **112**, 147-51.